



UNIVERSITY OF LEEDS

This is a repository copy of *Non-woven fabric activated carbon produced from fibrous waste biomass for sulphur dioxide control*.

White Rose Research Online URL for this paper:
<http://eprints.whiterose.ac.uk/140515/>

Version: Accepted Version

Article:

Illingworth, JM, Rand, B and Williams, PT orcid.org/0000-0003-0401-9326 (2019)
Non-woven fabric activated carbon produced from fibrous waste biomass for sulphur dioxide control. *Process Safety and Environmental Protection*, 122. pp. 209-220. ISSN 0957-5820

<https://doi.org/10.1016/j.psep.2018.12.010>

© 2018 Institution of Chemical Engineers. Published by Elsevier B.V. All rights reserved.
This manuscript version is made available under the CC-BY-NC-ND 4.0 license
<http://creativecommons.org/licenses/by-nc-nd/4.0/>.

Reuse

This article is distributed under the terms of the Creative Commons Attribution-NonCommercial-NoDerivs (CC BY-NC-ND) licence. This licence only allows you to download this work and share it with others as long as you credit the authors, but you can't change the article in any way or use it commercially. More information and the full terms of the licence here: <https://creativecommons.org/licenses/>

Takedown

If you consider content in White Rose Research Online to be in breach of UK law, please notify us by emailing eprints@whiterose.ac.uk including the URL of the record and the reason for the withdrawal request.



eprints@whiterose.ac.uk
<https://eprints.whiterose.ac.uk/>

Non-woven fabric activated carbon produced from fibrous waste biomass for sulphur dioxide control

James M. Illingworth, Brian Rand, Paul T. Williams *

School of Chemical & Process Engineering
University of Leeds, Leeds, LS2 9JT, UK

* (Corresponding author; Email: p.t.williams@leeds.ac.uk; Tel. ##44 113 3432504)

ABSTRACT: Waste fibrous biomass (flax) has been processed using non-woven textile techniques to produce a fibrous fabric material. The biomass fabric was then processed to produce activated carbons which retained their structure and flexibility. The carbons produced in a range of process conditions possessed a range of different surface areas and porosities. The activated carbons produced by chemical activation at different temperatures had high surface areas, ranging from $126 \text{ m}^2 \text{ g}^{-1}$ for the activated carbon produced at $450 \text{ }^\circ\text{C}$ to $1177 \text{ m}^2 \text{ g}^{-1}$ produced at $800 \text{ }^\circ\text{C}$ activation temperature. At increased hold times at $800 \text{ }^\circ\text{C}$ the surface areas increased further, for example reaching $1656 \text{ m}^2 \text{ g}^{-1}$ at 2 h hold time. The activated carbons were found to be very microporous, containing very small micropores. The produced activated carbons were then investigated in terms of the removal of sulphur dioxide in a bench scale continuous flow reactor. The SO_2 adsorption results showed that for the waste biomass fibre carbons, uptake of SO_2 from the gas stream was found to be dependent on the degree of activation. As the micropore volume and surface area of the samples increased, the SO_2 adsorption capacity also increased, observing a linear relationship. The adsorption of SO_2 by the waste derived activated carbons was significantly higher when compared to commercially obtained activated carbons. This appeared to be related to the pore size distribution of the samples, with the waste biomass activated carbons possessing a greater number of ultra-micropores than the commercial samples. Increase in the temperature of the activated carbon bed led to a marked decrease in the adsorption of SO_2 . Uptake of SO_2 was also shown to be dependent on the concentration of the SO_2 inlet feed gas, where higher SO_2 concentrations led to enhanced uptake. The advantages of using textile processing techniques to produce a non-woven fabric activated carbon enabling different forms to be produced related to the end-use application has great potential for resource recovery.

Keywords: Biomass; Waste; Activated carbon; Sulphur dioxide; Resource efficiency; Environment

1. Introduction

There is considerable current concern over the emissions of pollutants to the atmosphere from industrial processes. Sulphur dioxide emissions are of particular concern since it has a detrimental effects on human health and the environment and there are strict regulatory controls of emissions of SO₂ from industrial processes (Xu et al, 2016). For example, the European Industrial Emissions Directive (EC, 2010) covers SO₂ emissions (and other emissions) from a range of large plants including coal fired power plant, cement kilns, steel industry, waste incinerators etc. The most common methods for control of sulphur dioxide involve desulphurisation with reactants such as lime or limestone, or wet-scrubbing with alkalis such as calcium hydroxide or sodium hydroxide (Karatepe, 2000; Sun et al., 2016). However, there is growing interest in the use of activated carbon for control of SO₂ due to advantages which include high operational flexibility and lower maintenance costs (Karatepe, 2000; Xu et al, 2016).

Activated carbons are high surface area, high porosity materials with a high surface activity and mechanical strength which are widely used in industrial applications (Yahya et al., 2015). Biomass waste in the form of agricultural waste materials have been extensively investigated as precursors for the production of activated carbons (Yahya et al, 2015, Koseoglu and Akmil-Basar, 2015; Ioannidou and Zabaniotou, 2007). For example, cotton stalks (Nahil and Williams, 2012) date stones (Al-Rahbi et al, 2016), coconut shell (Hu and Srinivasan, 1999) palm shell (Daud et al, 2000) rice bran (Suzuki et al, 2007), corn cobs (El-Hendawy et al., 2001) rice husks (Yalcin and Sevine, 2000) etc.

The adsorptive properties of such waste derived activated carbons have been utilised as pollution control materials for control of polluting gases. For example, Al-Rahbi et al (2016) used waste biomass in the form of date stones to produce activated carbons for the low

temperature (50 °C) control of NO_x. They reported that the biomass derived activated carbon had similar removal efficiencies for NO_x as for commercially available activated carbons and that the micropore structure of the carbon significantly influences removal efficiency. Porosity classification of activated carbons have been defined by the International Union of Pure and Applied Chemistry (IUPAC) as micropores (pore size <2 nm) mesopores, (2-50 nm) and mesopores (>50 nm) (Yahya et al, 2015). Very small micropores have also been defined as ultra-micropores with pore size < 0.5 nm. Lee et al (2002) prepared activated carbons via the chemical activation of coconut shells and investigated their use for the removal of SO₂ in a fixed bed reactor. They reported that the adsorption of SO₂ was influenced by the alkali used in the chemical activation (KOH) through chemical adsorption. Katada et al (2003) investigated the removal of sulphur dioxide using activated carbons produced from several waste biomass, including waste urban wood and coconut shells in a fixed bed reactor at low temperature (45 °C). They reported high removal efficiencies for some of the biomass derived activated carbons (>90%) which they attributed to the pore structure, surface chemistry and hydrophobic/hydrophilic properties of the carbons. Guo and Lua (2003) also used a fixed bed reactor system to study the adsorption of sulphur dioxide in nitrogen onto activated carbons produced from waste biomass in the form of oil-palm shells. They reported that the uptake of the sulphur dioxide was dependent on the operating conditions of the reactor (particularly SO₂ flow rate), the textural characteristics (particle size and porosity) of the carbon and the surface chemistry of the activated carbon.

Activated carbons are produced using either physical activation or chemical activation (Yahya et al, 2015). Physical activation is a two-stage process, firstly involving pyrolysis of the biomass agricultural waste material (typically at ~ 500 °C) in an inert atmosphere which produces a char. The char is then activated via partial oxidation with air, steam or carbon dioxide to produce the activated carbon (typically at ~700-900 °C). Chemical activation

involves impregnation of either the biomass precursor or the pyrolysis char with the chemical activating agent (typically used are KOH, NaOH, HNO₃, H₃PO₄, ZnCl₂) followed by activation in an inert atmosphere at temperatures which can range from 300 – 800 °C. The chemicals acting as dehydrating agents and oxidants to aid pore development in the carbon. A final stage involves washing of the product activated carbon to remove the residual activating chemicals.

For particular control of sulphur dioxide, activated carbon in the form of activated carbon fibres have been shown to be effective for control of SO₂ from flue gases (Mochida et al, 2000; Mangun et al, 2001; Daley et al., 1997; Davini 2003; Gaur et al, 2006). For example, Magnun et al (2001) used activated carbon fibres with different surface areas (730 – 1890 m² g⁻¹) prepared from a woven phenolic fibre and steam/CO₂ activation for the adsorption of SO₂ at 120 °C. They reported that SO₂ adsorption was influenced by pore size and the basicity of the carbon surface groups, but there was less influence of surface area. Davini (2003) used activated carbon fibres produced from polyacrylonitrile fibres and CO₂ activation for control of SO₂ from a simulated mixture of flue gases at a temperature between 100 and 160 °C. Surface chemistry, i.e. the presence of nitrogen groups from the acrylonitrile precursor were found to influence the amount of SO₂ adsorbed. Commercially produced activated carbon fibre is produced via a synthetic process. For example, the raw material such as acrylonitrile or coal tar pitch is polymerised and spun to produce fibres which are then oxidised and activated to produce the activated carbon fibre (Mochida et al, 2000). It has been reported that such synthetically activated carbon fibres have superior adsorption ability compared to granular activated carbons. This has been ascribed to the micropores in the carbon fibres which open directly onto the surface of the carbon rather than being located within mesopores or transitional pores (Mochida et al, 2000). In addition, the small size of the fibres facilitates gas/liquid to solid interaction (Gaur et al, 2006). However, synthetically produced activated carbon fibres are more expensive (Mochida et al, 2000). Therefore the production of activated

carbon fibres from fibrous biomass waste which have good adsorptive properties for pollutants would be of significant economic potential.

A particular type of biomass waste is fibrous biomass which has also been investigated for the production of activated carbons (Dizbay-Onat et al, 2017; Shamsuddin et al, 2016; Hwang et al, 2015; Zhao et al. 2015). The fibrous nature of the biomass waste material has been utilised in our previous work to produce a non-woven textile fabric matting which is then processed to produce activated carbon that retains its original fabric matting structure after activation (Illingworth et al, 2012; Williams and Reed, 2003; 2004). The process has the potential for the fibrous biomass to be produced via textile technology into a variety of pre-formed shapes. Thereby the activated carbon fabric matting can be used directly in various end-use applications, rather than the need for further processing such as granulation of the carbon, cartridge packing or attachment to a support.

There are few studies reporting on the use of activated carbon fibrous material produced from biomass fibrous waste material and none related to the adsorption of SO₂ using processed activated carbon fabric matting. In this paper we report on the production of activated carbon fabric matting using physical and chemical activation for the adsorption of SO₂. Different process conditions for the production of the activated carbon matting have been used and their influence on SO₂ adsorption investigated. The adsorption results are compared with that obtained using commercially available activated carbons.

2. Materials and methods

2.1 Materials

The precursor biomass material used for the production of the non-woven biomass fabric was a low-grade flax fibre obtained from British Fibres Limited, UK. The raw flax was prepared using a 'scutching' process which separates the woody flax stems from the surface of the fibres producing the raw material for the experiments which consisted of long flax fibres, shorter coarse fibres and surface woody material. The produced flax fibre was then processed into a non-woven fabric material. The process involved aligning the fibres into parallel arrays using rotating cylinders covered with small wires. The position of the wires can be modified during the process to alter the direction in which the fibres are laid, thereby providing a greater cross directional strength within the fabric. The flax material was produced at a uniform thickness of 8mm. The fabric was then subjected to needle-punch bonding, whereby, barbed needles are punched through the fabric, hooking and tangling the fibres together, enhancing the strength and stability of the non-woven fabric. Finally, the material was rolled between two heated cylinders where the heat and pressure causes the fibres to fuse, further adding to the structural stability of the non-woven fabric. Figure 1 shows a photograph of the non-woven fibrous flax fabric material.

For comparison of the effectiveness of the produced activated carbons in relation to their effectiveness for SO₂ adsorption, three commercial activated carbons were used for comparison. These were an activated carbon fibre from the Osaka Gas Company, Japan), a granular lignite carbon from BDH Ltd., UK, and a powdered carbon (Darco) obtained from Sigma Aldrich Ltd.

2.2. Production of activated carbons

The production of activated carbon involved mainly chemical activation through pyrolysis of the flax biomass material followed by chemical impregnation of the char and activation at

temperatures between 450 °C and 800 °C. In addition, samples of activated carbon were prepared by physical activation, involving production of the pyrolysis char followed by activation in carbon dioxide. The pyrolysis of the non-woven flax fabric material was carried out in a bench scale static-bed batch reactor, the details of which have been reported in our earlier work (Illingworth et al., 2012). The reactor was constructed of stainless steel (length 200mm, internal diameter 65mm) which enabled the pyrolysis of up to 60 grams of biomass material. The reactor was heated by an electrically heated vertical furnace (length 300 mm, internal diameter 75mm). Nitrogen was used as the purge gas to maintain pyrolysis conditions. The samples of biomass non-woven material were heated at a heating rate of 2 °C min⁻¹ to the final pyrolysis temperature of 800 °C and held at that temperature for 60 mins.

Chemical activation of the pyrolysis chars was the method used to produce the activated carbons. The product non-woven flax char material derived from pyrolysis was dried overnight at 110°C and 1.00g quantities were then thoroughly mixed with 50ml of deionised water containing potassium hydroxide as the activating chemical. The ratio of mass of KOH to mass of char was 4:1. The mixture was then evaporated to dryness at 80°C before drying at 110°C for 24 hours. The impregnated chars were then heated at 5°C min⁻¹ to the activation temperatures of either 450 °C, 650 °C or 800 °C without any hold time under a nitrogen flow using the same reactor used for pyrolysis. In addition, hold times at 800 °C were also increased to 1 and 2h. After the activation procedure, the carbons were washed with water to remove the residual KOH until the wash water attained a pH of 7 to 7.5. The product activated carbons were finally dried at 110°C for 24 hours. A typical non-woven fibrous activated carbon fabric material produced by pyrolysis followed by activation using KOH is shown in Figure 2. Examination of the activated carbon produced by chemical activation by scanning electron microscopy (Figure 3) also showed the fibrous nature and fibre shape and structure of the original flax biomass waste had been retained after the chemical activation procedure.

In addition, physical activation of the flax pyrolysis chars was carried out to produce activated carbons to compare with the activated carbons produced via chemical activation. The pyrolysis chars produced from the non-woven flax material were heated at $5\text{ }^{\circ}\text{C min}^{-1}$ to a final temperature of $825\text{ }^{\circ}\text{C}$ under a nitrogen flow using the same reactor used for pyrolysis. The nitrogen flow was then switched to CO_2 which acted as the activation gas. Carbon dioxide activation was carried out at $825\text{ }^{\circ}\text{C}$ for 6 h.

2.3. Characterisation of surface area and porosity of activated carbons

The surface area and porosities of the product activated carbons was determined using a Quantachrome Autosorb 1-C Instrument. All chars were outgassed prior to analysis and nitrogen adsorption isotherms were determined over a range of relative pressures from 1×10^{-6} to 0.995 and desorption isotherms were measured down to a partial pressure of 0.10. The surface area of the activated carbons was calculated using the BET procedure and the total micropore volume using the Dubinin-Radushkevitch (DR) equation (DR-N_2). The Dubinin-Radushkevitch equation was used to provide an assessment of the volume of very small ultra-micropores (DR-CO_2) (pore size $<0.7\text{ nm}$) from adsorption isotherms of CO_2 produced at 273 K over the relative pressure range 1×10^{-6} to 0.03. Micropore size distributions were constructed using the Density Functional Theory (DFT) software supplied by Quantachrome Ltd.

2.4. Sulphur Dioxide Adsorption System

The SO_2 adsorption experiments using the product activated carbons and the commercially obtained activated carbons were investigated using a continuous flow reactor (Figure 4). The reactor was constructed of stainless steel (120 mm length, 20 mm diameter) and was heated

externally by an electrical furnace. A standard SO₂ gas mixture was purchased from BOC Gases Ltd. UK and contained 5000 ppm SO₂ balanced by nitrogen. The gas could be mixed with additional nitrogen to produce different concentrations of SO₂ for the adsorption experiments. The flow of gases was measured by calibrated rotameters. To ensure efficient mixing of the gases prior to the sample bed, the top half of the reactor unit was packed with stainless steel grommets.

A sample (250 mg) of the activated carbon was mixed with 5.00g of sand in a removable sample holder to give a bed depth of ~15 mm and was dried at 120 °C for 2 hours prior to the SO₂ adsorption experiments. This dispersed bed configuration was used to minimise pressure drop differences (Li et al. (2002)). Initial experiments showed that the adsorption of SO₂ on the sand was insignificant. The sample bed of activated carbon was fixed in position by fine wire gauze and glass fibre filters to prevent channelling of the gas flow through the bed. For all breakthrough experiments, time zero was defined as the time taken for the outlet SO₂ concentration to equal the inlet concentration with the sample bed containing only sand. The SO₂ laden gas was then passed through the carbon bed and the outlet concentration was measured on-line using an Analytical Development Company Ltd, UK infrared SO₂ gas analyser (ppmv). In all cases, the gas flow rate was maintained at 300ml min⁻¹ which was the minimum flow accepted by the on-line analyser. The adsorption was performed until the bed reached saturation, i.e. the outlet concentration becoming equal to the inlet concentration.

Following the experiments, breakthrough curves could then be plotted and the total amount of SO₂ adsorbed calculated. The mass of SO₂ passing through the sample bed between each measurement period (1 minute) can be calculated according to equations 1 - 3:

$$Q_{SO_2} = (V_{SO_2} / 100) \times Q \quad (1)$$

where: Q_{SO_2} = flow of SO₂ through sample bed (l min⁻¹)

V_{SO_2} = vol% of SO_2 in feed gas

Q = total flow of gas through sample bed ($l \text{ min}^{-1}$)

$$\text{then } M_{SO_2} = (Q_{SO_2}/24.04) \times RMM_{SO_2} \quad (2)$$

where: M_{SO_2} = mass of SO_2 passing through sample bed ($g \text{ min}^{-1}$)

RMM_{SO_2} = relative molecular mass of SO_2 ($64g \text{ mol}^{-1}$)

therefore, the mass of SO_2 adsorbed over each measurement period may be defined as:

$$A_{SO_2} = M_{SO_2} \times \left[1 - \frac{C/C_{0(t)} + C/C_{0(t+1)}}{2} \right] \quad (3)$$

where: A_{SO_2} = mass of SO_2 adsorbed over 1 minute measurement period (g)

$C/C_{0(t)}$ = ratio of outlet concentration/inlet concentration of SO_2 at time t

$C/C_{0(t+1)}$ = ratio of outlet concentration/inlet concentration at time t + 1 minute

The total mass of SO_2 adsorbed during a breakthrough experiment can then be calculated as follows:

$$A_{TOT} = (\sum A_{SO_2}) \times 1/W_C \quad (4)$$

where: A_{TOT} = total mass of SO_2 adsorbed ($g \text{ gC}^{-1}$)

W_C = mass of carbon sample in fixed bed (g)

3. RESULTS AND DISCUSSION

3.1 Surface area and porosity characteristics of the activated carbons

Density Functional Theory (DFT) software was used to determine the micropore size distributions of the produced activated carbons and the commercially obtained carbons. Figure

5 shows the DFT-N₂ and DFT-CO₂ for the produced carbons and Figure 6 for the commercially obtained carbons respectively. For the produced carbons (Figure 5), there is considerable pore development during the activation process compared to the pyrolysis char. In particular the micropores of <7 Å and ultra-micropores of <4 Å show significant increase as the activation temperature was increased. It is also noteworthy that for longer time duration at 800 °C activation temperature of 1 h and 2 h, the carbons show the presence of larger pores of >7 Å suggesting degradation of pore walls and pore widening. Figure 6 shows the DFT micropore size distributions of the commercially obtained carbons. The results suggest that the commercially obtained activated carbons have a lower pore size distribution below 7 Å, and significantly less of the ultra-micropores of <4 Å.

Table 1 shows the surface area and porosity characteristics of the intermediate pyrolysis char and activated carbons produced in this work and the commercially obtained activated carbons. The char produced from pyrolysis of the non-woven flax fabric material had a relatively low surface area of 30 m² g⁻¹ and low microporosity. The influence of chemical activation showed an improvement in surface area and development of microporosity in the product activated carbons. The influence of chemical activation at 450 °C activation temperature was modest, but at higher temperatures the development of surface area and porosity became very marked, such that at 800 °C and no hold time the surface area reached 1177 m² g⁻¹ and micropore volume (DR-N₂) reached 0.451 cm³ g⁻¹. It is also noteworthy that the yield of the activated carbon product was 83 wt.% at 800 °C activation temperature and no hold time. Increasing the hold time at 800 °C produced very high surface area activated carbon, at 1564 m² g⁻¹ and 1 h hold time and 1656 m² g⁻¹ at 2 h hold time and also increased micropore volumes, however, activated carbon yields decreased to 67 wt.% and 57 wt.% respectively. The activated carbon produced via physical activation had much lower surface area and lower micropore volume and lower yield compared with the chemically activated carbons. Table 1

also shows the properties of the commercially obtained activated carbons, notable is the high surface area of the activated carbon fibres ($1715 \text{ m}^2 \text{ g}^{-1}$) and high microporosity ($0.633 \text{ cm}^3 \text{ g}^{-1}$ pore volume).

3.2. SO₂ adsorption by the activated carbons

Figure 7 shows the SO₂ breakthrough curves and Figure 8 shows the cumulative SO₂ adsorption profiles for the pyrolysis char and the activated carbons produced by chemical and physical activation of the flax non-woven fabric material. Also shown are the SO₂ breakthrough curves and cumulative SO₂ adsorption profiles for the commercially obtained activated carbons. Not tested was the chemically activated carbon at 2 h hold time at 800 °C as the surface area and porosity characteristics were similar to the activated carbon produced at 1 h hold time. The SO₂ adsorption tests were carried out at a reaction temperature of 25 °C and with an SO₂ concentration of 2500ppm, balanced by nitrogen.

The commercially obtained activated carbons showed similar overall adsorptive capacities for SO₂ even though there were large differences in the BET surface area and micropore volume. However, the characteristics of the microporosity as determined by CO₂ adsorption at 273K were similar for the three commercial activated carbons. This seems to suggest, at the low partial pressures of SO₂ employed, that the adsorption was taking place primarily in the ultra-micropores. Although the adsorption capacity was similar, the rate at which equilibrium was obtained varied considerably. Figure 8 shows that activated carbon fibre and powder samples showed the most rapid adsorption, and that saturation of the carbon adsorption bed was reached in 13 and 16 minutes respectively. The granular activated carbon showed the slowest rate of adsorption where equilibrium was reached at 23 minutes. This is most probably related to the slower rates of diffusion of the SO₂ to the adsorption sites away

from the surface of the carbon granules. The smaller dimensions of the activated carbon fibre (15-20 μm) and powder (ca. 100 μm) would allow more efficient access to the adsorption sites. Lua and Guo (2001) examined the effect of particle size on the uptake of SO_2 with physically activated carbons obtained from oil-palm stones. They found that an increase in particle size (from 1.0-2.0mm to 2.8-4.0mm) had no effect on the total amount of SO_2 adsorbed but the time taken to reach saturation increased from ~40 to ~80 minutes. It was concluded that the larger the particle size the longer would be the time required for the SO_2 molecules to diffuse into the pore sites.

Figures 7 and 8 also show the SO_2 breakthrough curves and the cumulative SO_2 adsorption profiles for the pyrolysis char and also the activated carbons prepared by chemical activation with KOH, and the physically activated carbon. The pyrolysis char exhibited a significant SO_2 adsorption capacity, representing ~70% of the total adsorption of the commercial activated carbons. The isotherms of carbon dioxide at 273K allow a more accurate assessment of the ultra-micropores (DR- CO_2). The critical molecular dimensions of N_2 and CO_2 gases are similar, however the CO_2 molecule has far greater kinetic energy at 273K than N_2 at 77K, thus facilitating entry to very fine pores of molecular dimensions. The uptake of CO_2 by the pyrolysis char as evidenced by the DR- CO_2 data of Table 1 suggests that although inaccessible to N_2 at 77K, the flax pyrolysis char shows considerable uptake of CO_2 at 273K indicating the presence of ultra-micropores. These very small micropores would be more accessible to SO_2 at the temperatures used in this study as the dimensions of the two molecules are quite similar (3.90 \AA for CO_2 , 4.29 \AA for SO_2 (Harrison, 1977) as shown in Figure 7.

Figures 7 and 8 show that for the series of chemically activated carbons produced from the biomass waste flax, non-woven fabric there was a data trend of increasing SO_2 adsorption as the degree of activation in terms of the activation temperature and hold time at the activation temperature was increased. That is, the activated carbon produced by chemical activation with

KOH at 800 °C and with a hold time of 1 h produced the highest uptake of SO₂. The chemically activated carbon produced at 450 °C had a similar adsorption capacity to the pyrolysis char but showed more rapid uptake in the initial stages of the experiment, suggesting a slight widening of porosity during the activation process allowing increased access to the adsorption sites. As the activation temperature was raised to 650 °C and further to 800 °C, a large increase in SO₂ adsorption was observed coinciding with a substantial increase in the micropore volume as shown by the DR-N₂ micropore volume data of Table 1. The increase in capacity was less marked for the 800 °C (1hr) activated carbon sample despite a significant increase in the wider micropore volume (DR-N₂). However, the very small micropore volume (DR-CO₂) showed only a slight increase, again indicating that the adsorption is taking place mainly in the ultra-micropores. The time taken to establish equilibrium (Figure 8) for the chemically activated carbons was generally longer than for the commercially obtained activated carbon powder and fibre samples. However, the overall adsorption capacity for SO₂ was much higher for the waste derived flax non-woven activated carbon fabric samples. The flax non-woven fabric activated carbon produced by physical activation showed similar SO₂ adsorption to the 650 °C KOH chemically activated carbon sample, both of which had similar values for the very small micropore volume (DR-CO₂).

The relationship between the BET surface area and uptake of SO₂ (from Figure 8) is shown in Figure 9. When all of the activated carbon samples investigated are plotted, there was little relationship between the surface area and the SO₂ capacity of the samples. However, when considering only the KOH chemically activated series of biomass waste derived activated carbons, a good correlation was observed. It is suggested that this is due to the fibrous nature of the chemically activated carbons and the high proportion of the very small ultra-micropores present in these activated carbons, which make up a substantial proportion of the surface area.

Figure 10 shows the relationship between SO₂ adsorption capacity and the micropore volume for all of the activated carbon samples examined. There appears to be very little correlation between the SO₂ uptake (from Figure 8) of the samples and the micropore volume as determined by N₂ adsorption (DR-N₂). In contrast, an improved correlation was observed between the SO₂ uptake and the micropore volume measured by CO₂ adsorption (DR-CO₂). This correlation was improved considerably when the commercially obtained activated carbon samples were omitted from the data, with an r^2 value above 0.99. This suggests a linear relationship between the ultra-micropore volume as assessed by CO₂ adsorption, and the SO₂ adsorption capacity.

A further factor which would influence uptake of SO₂ of the chemically activated carbons is the surface chemistry of the carbons. Activation with an alkali activating agent in the form of KOH would lead to an increase in the basicity of the carbon surface (Xu et al. 2016). The alkaline surface properties would enhance the adsorption of the acidic gas SO₂. Xu et al. (2016), have also noted that char produced from pyrolysis of biomass is quite alkaline with pH values >8, suggesting that the high activity of the flax non-woven biomass pyrolysis char for SO₂ adsorption shown in this work may also be due to the alkaline properties of the char. In addition, the presence of surface oxygen in the form of oxygen-containing functional groups would enhance SO₂ uptake (Li et al, 2001, Karatepe et al, 2008).

The adsorption capacities of the non-woven fabric material produced from the flax biomass waste are similar to other reported data. For example, Guo and Lua (2002) examined SO₂ adsorption (2000 ppm in nitrogen) on oil palm-shell based activated carbons activated under various conditions. For a given surface area, KOH activated palm-shell chars produced higher SO₂ capacities than physically activated carbons from the same precursor. Uptake of SO₂ by the KOH activated carbons ranged from ~30 – 70 mg SO₂/gC as the surface area was increased from 350-1400 m² g⁻¹, with a linear trend observed. The authors suggested that the

enhanced uptake of SO₂ by the KOH activated carbons was due to the presence of sub-micropores that were accessible to SO₂ at room temperature.

The particular characteristics of the non-woven fabric activated carbon material would also enhance SO₂ uptake, because of the fibrous nature of the activated carbon. Because of the micron-sized (typically 5 – 20 µm) fibres (Figure 3), the particle size mass transfer resistance is almost negligible (Gaur et al, 2006)

3.3. Influence of process parameters on SO₂ adsorption by the activated carbons

The influence of activated carbon temperature and SO₂ gas concentration in the inlet gases on adsorption of SO₂ by the biomass waste derived activated carbons was investigated. The influence of temperature was investigated using the activated carbon produced at 800 °C using chemical activation with KOH at reactor temperatures of 25 °C, 40 °C and 100 °C. The SO₂ breakthrough curves and the cumulative SO₂ adsorption profiles for the activated carbon in relation to temperature are shown in Figure 11 and Figure 12 respectively. The results show clearly that there is a marked reduction in the SO₂ breakthrough time period as the temperature of the reactor was increased, similarly the adsorption capacity of the carbon was rapidly reduced as the temperature was increased to 100 °C. Karatepe et al, (2008) also showed that increasing the activated carbon adsorption temperature from 25 °C to 50 °C resulted in a significant decrease in the adsorption of SO₂ for activated carbon produced from lignite. They suggested that the reduction was due to the fact that during the adsorption process, the molecules of SO₂ lose their kinetic energy resulting in an exothermic process. Therefore, increasing the adsorption temperature produces lower SO₂ adsorption.

The effect of varying the inlet gas concentration of SO₂ on the adsorption capacity of the activated carbon produced at the activation temperature of 800 °C using chemical activation with KOH was investigated. Breakthrough experiments were carried out with SO₂ concentrations of 750, 2500 and 5000ppm in the inlet feed gas. The breakthrough curves and cumulative SO adsorption results are shown in Figures 13 and 14 respectively. For all samples, the uptake of SO₂ increased significantly as the concentration in the feed was increased and more rapid breakthrough was also observed. Similar trends were observed by Lua and Guo (2001) as they varied the SO₂ inlet gas concentration from 500 to 2000 ppm for activated carbons produced from oil-palm stones. Karatepe et al. (2008) also showed that higher concentrations of SO₂ inlet gas led to higher adsorption of SO₂ onto activated carbon produced from lignite.

Overall the research has shown that activated carbons in the form of a non-woven fabric material can be produced from biomass fibrous waste. The production of activated carbons in the form of textiles, cloths or composites offers materials that are much easier to handle when compared with loose fibre or powder forms. Non-woven fabrics are strong, adsorbent and stretchable and can be produced at significantly lower cost than woven textiles. For this study, the material was produced at a uniform thickness of 8mm, although the thickness and weights of the non-woven fibrous biomass waste can be adjusted to particular requirements. The research reported here has also shown that the product activated carbon retains the original structure of the precursor raw fabric material. Therefore, the fibrous flax waste biomass could be processed using the described textile techniques to produce a precursor fabric material which could be formed to produce a wide variety of dimensions and shapes, related to the end-use application of the activated carbon. Activated carbon was produced by a chemical activation process using KOH under different process conditions and compared with the properties and adsorption capacity of physically activated carbon. Chemical activation has some advantages

over physical activation in that higher surface areas are produced (Yahya et al, 2015). For example, the product activated carbon had very high surface areas of up to $1656 \text{ m}^2 \text{ g}^{-1}$ and where shown to possess a high proportion of very small micropores. The microporous nature of the activated carbons, coupled with their high surface area made for effective adsorption of SO_2 under the test conditions used in this study. The adsorption of SO_2 from the waste derived activated carbons was found to be similar and in some cases significantly better than the results obtained with commercially obtained activated carbons. The process of producing activated carbons that can be manipulated and formed into different shapes, sizes and thickness to suit different waste flue gas (or waste water) cleaning applications has great potential. In addition, commercial activated carbons are produced from precursors such as wood, but also include non-renewable fossil fuel sources such as coal, peat and lignite (Yahya et al. 2015). In the particular case of activated carbon fibres, these are mainly produced from viscose-cellulose, petroleum pitch fibre and polyacrylonitrile resin fibre (Li et al, 2015). Using a biomass based waste material such as the agricultural fibrous waste flax would represent a more sustainable feedstock but also produces a high quality activated carbon product from a waste as an exemplar of resource recovery.

Whilst an activated carbon produced from waste material for control of a pollutant is environmentally attractive, the activated carbon becomes saturated and loses efficiency for SO_2 capture and therefore the management of the used activated carbon which contains the trapped SO_2 , mainly as H_2SO_4 , (Zhang et al. 2012) would be an issue. Therefore, an integrated pollution prevention and control approach would require consideration of the regeneration or disposal of the used activated carbon. Salvador et al. (2015a; 2015b) have recently undertaken an extensive review of the regeneration processes used for used activated carbons. The main methods of regeneration include thermal processes (Salvador et al, 2015a) and chemical, microbiological and vacuum processes (Salvador et al. 2015b). The regeneration process ideally removes the

pollutant whilst maintaining the porous structure of the activated carbon for subsequent re-use. For the regeneration of SO₂-saturated activated carbon, the common methods for regeneration are water scrubbing or thermal treatment. However, water scrubbing requires large amounts of water and thermal methods require energy input and also consumes some of the carbon (Zhang et al. 2012). Eventually the adsorption efficiency of the activated would become lowered after several regenerations due to damage to the pore structure of the activated carbon and therefore disposal becomes the treatment option. However, the SO₂ could be removed from the activated carbon and would thereby produce a bio-char material which could be used as a soil enhancer which improves soil retention of nutrients and agrochemicals for plant and crop utilization (Windeatt et al, 2014). More nutrients stay in the soil instead of leaching into groundwater and causing pollution. The bio-chars are added to soil to hold the carbon from the original biomass in the soil and therefore act as a carbon sequestration process.

4. Conclusions

Fibrous waste flax biomass has been processed using textile techniques to produce a non-woven fabric material. The non-woven fabric was activated using pyrolysis-chemical activation with KOH at various temperatures to produce an activated carbon which were examined for their surface area and porosity characteristics. The characteristics of the carbons were compared with a physically activated waste flax biomass prepared activated carbon and with three commercially obtained activated carbons. The waste derived activated carbons showed increased surface area and microporosity as the severity of the activation procedure was increased. For example, the activated carbon produce at an activation temperature of 450 °C had a surface area of 126 m² g⁻¹ and a micropore volume (DR-N₂) of 0.05 cm³ g⁻¹. However at 800 °C activation temperature, the surface area was markedly increased to 1177 m² g⁻¹.

Increasing the hold time to 2 h at 800 °C produced a carbon with a high surface area of 1656 m² g⁻¹ and a high degree of micropores, at 0.639 cm³ g⁻¹ pore volume (DR-N₂).

The product waste derived non-woven fabric activated carbons were examined in relation to their ability to adsorb SO₂ from a continuous gas flow. The high surface area and microporous nature of the waste derived activated carbons was crucial in allowing the carbons to adsorb large amounts of SO₂. The micropores (<2 nm) included a high proportion of very small micropores allowing the small SO₂ molecule of dimension 0.429 nm to easily enter the pores of the activated carbon. There was a good correlation between the uptake of SO₂ and surface area for the series of activated carbons produced by KOH chemical activation. In relation to the microporosity, there was a good correlation between the microporosity and SO₂ uptake for the chemically activated waste derived activated carbons using N₂ adsorption data (DR-N₂) However, for the small micropores determined using CO₂ adsorption (DR-CO₂) which measures the smaller micropores, there was a very good correlation between the ultra-micropores and SO₂ uptake with an r² value above 0.99. This suggests a linear relationship between the very small micropore volume as assessed by CO₂ adsorption, and the SO₂ adsorption capacity (CO has a molecular size of 0.39 nm compared to SO₂ at 0.429 nm. The SO₂ adsorption performance of the waste derived activated carbons was compared with three commercially obtained activated carbons. For the activated carbons produced at 800 °C with KOH chemical activation, the SO uptake was greater compared to the commercially activated carbons, attributed to the large proportion of ultra-micropores. Increasing the reactor temperature to 100 °C resulted in a marked decrease in the uptake of SO₂ by the activated carbons. Also, higher SO₂ concentrations in the inlet gas produced an increase in the amount of SO₂ adsorbed.

The process of producing activated carbons from a fibrous waste biomass have been demonstrated, particularly since the fibrous biomass can be processed into non-woven fabric

material which retains its structure and flexibility after activation. Therefore manipulation of the process can produce an activated carbon of differing structure, thickness and form directly related to the requirements of the end-use application. The product activated carbons produced by chemical activation using KOH have been shown to have high surface area with ultra-micropores which are effective for SO₂ adsorption.

ACKNOWLEDGEMENTS

A scholarship from the UK Engineering & Physical Sciences Research Council is gratefully acknowledged for one of us (JMI)

REFERENCES

- Al-Rahbi A.S., Nahil M.A., Wu C., Williams P.T. 2016, Waste derived activated carbons for control of nitrogen oxides. *Waste Resour. Manag.* 169, 30-41.
- Daud W.M.A.W., Ali W.S.W., Suleiman M.Z. 2000. The effects of carbonization temperature on pore development in palm-shell based activated carbon. *Carbon*, 38, 1925-1932.
- Davini P. 2003. Flue gas desulphurisation by activated carbon fibres obtained from polyacrylonitrile by-product. *Carbon*, 41, 277-284.
- Dizbay-Onat M., Vaidya U.K., Lungu C.T. 2017. Preparation of industrial sisal fiber waste derived activated carbon by chemical activation and effects of carbonization parameters on surface characteristics. *Ind. Crops Prod* 95, 583-590.
- EC Industrial Emissions Directive, 2010. 2010/75/EU. European Commission, Brussels.
- El-Hendawy A.N.A., Samra S.E. Girgis B.S., 2001. Adsorption characteristics of activated carbons obtained from corncobs. *Colloid Surface A*. 180, 209-221.
- Gaur V. Asthana R., Verma N., 2006. Removal of SO₂ by activated carbon fibres in the presence of O₂ and H₂O. *Carbon* 44, 46-60.
- Guo, J., Lua, A.C. 2002. Textural and chemical characterisations of adsorbent prepared palm shell by potassium hydroxide impregnation at different stages. *J. Colloid Interfac. Sci.* 254(2), 227-233.
- Guo J., Lua A.C. 2003. Adsorption of sulphur dioxide onto activated carbon prepared from oil-palm shells with and without pre-impregnation. *Sep. Purif. Technol.* 30, 265-273.
- Harrison, R.D.(ed) 1977. Nuffield Advanced Science Book of Data, Longman Group, London.
- Hu Z. Srinivasan M.P. 1999. Preparation of high surface area activated carbons from coconut shell. *Micropor. Mesopor. Mater.* 27, 11-18.
- Hwang K.J., Park J.Y., Kim Y.J., Kim G. Choi C., Jin S., Kim N., Lee J.W., Shim W.G. 2015. Adsorption behaviour of dyestuffs on hollow activated carbon fiber from biomass. *Sep. Sci. Technol.* 50, 1757-1767.
- Illingworth J., Williams P.T. Rand B. 2012. Novel activated carbon fibre matting from biomass fibre waste. *Waste Resour. Manag.* 165, 123-132.
- Ioannidou O., Zabaniotou, A. 2007. Agricultural residues as precursors for activated carbon-A review. *Renew. Sus. Energ. Rev.* 11, 1966-2005.
- Karatepe N. 2000. A comparison of flue gas desulphurisation processes. *Energ. Sourc.* 22, 197-206.

- Karatepe N., Orbak I., Yavuz R., Oxyuguran A. 2008. Sulfur dioxide adsorption by activated carbons having different textural and chemical properties. *Fuel*, 87, 3207-3215.
- Katada N., Ii Y., Nakamura M., Niwa M. 2003. Oxidation of sulphur dioxide to sulphuric acid over activated carbon catalyst produced from wood. *J. Jpn. Pet. Inst.* 46, 392-395.
- Koseoglu E., Akmil-Basar C. 2015. Preparation, structural evaluation and adsorptive properties of activated carbon from agricultural biomass. *Adv. Powder Technol.* 26, 811-818.
- Lee Y.W., Park J.W., Choung J.H., Choi D.K. 2002. Adsorption characteristics of SO₂ on activated carbon prepared from coconut shell with potassium hydroxide activation. *Environ. Sci. Technol.* 36, 1086-1092.
- Li X., Ling L., Lu C., Qiao W., Liu Z., Liu L., Mochida I. 2001. Catalytic removal of SO₂ over ammonia-activated carbon fibers. *Carbon*, 39, 1803-1808.
- Li, Y.H., Lee, C.W., Gullett, B.K. 2002. The effect of activated carbon surface moisture on low temperature mercury adsorption. *Carbon*, 40(1), 65-72.
- Li J., Ng, D.H.L., Song P., Kong C., Song Y., Yang P. 2015. Preparation and characterisation of high-surface-area activated carbon fibers from silkworm cocoon waste for congo red adsorption. *Biomass Bioenerg.* 75, 189-200.
- Lua, A.C., Guo, J. 2001. Preparation and characterization of activated carbons from oil-palm stones for gas phase adsorption. *Colloid Surface A*, 179, 151-162.
- Mangun C.L., Debarr J.A., Economy J. 2001. Adsorption of sulphur dioxide on ammonia-treated activated carbon fibres. *Carbon*, 39, 1689-1696.
- Mochida I., Korai Y., Shirahama M., Kawano S., Hada T., Seo Y., Yoshikawa M., Yasutake A. 2000. Removal of SO_x and NO_x over activated carbon fibers. *Carbon* 38, 227-239.
- Nahil M.A., Williams P.T., 2012. Characterisation of activated carbons with high surface area and variable porosity produced from agricultural cotton waste by chemical activation and co-activation. *Waste Biomass Valorisation*, 3, 117-130.
- Rodriguez-Reinoso, F., Molina-Sabio, M. and Gonzalez, M.T. 1995. The use of steam and CO₂ as activating agents in the preparation of activated carbons. *Carbon*, 33(1), 15-23.
- Salvador F., Martin-Sanchez, N., Sanchez Hernandez R., Sanchez-Montero M.J., Izquierdo C. 2015a. Regeneration of carbonaceous adsorbents. Part 1: Thermal regeneration. *Micropor. Mesopor. Mat.* 202, 259-276.
- Salvador F., Martin-Sanchez, N., Sanchez Hernandez R., Sanchez-Montero M.J., Izquierdo C. 2015b. Regeneration of carbonaceous adsorbents. Part II: Chemical, microbiological and vacuum regeneration. *Micropor. Mesopor. Mat.* 202, 277-296.
- Shamsuddin M.S., Yusoff N.R.N., Sulaiman M.A. 2016. Synthesis and characterisation of activated carbon produced from kenaf core fiber using H₃PO₄ activation. *Procedia Chem.* 19, 558-565.

- Sun Y., Zwolinska E., Chmielewski A.G. 2016. Abatement technologies for high concentrations of NO_x and SO₂ removal from exhaust gases: A review. *Crit. Rev. Environ. Sci. Technol.* 46, 119-142.
- Suzuki R.M., Andrade A.D., Sousa J.C., Rollenberg M.C. 2007. Preparation and characterisation of activated carbon from rice bran. *Bioresource Technol.* 98, 1985-1991.
- Williams P.T., Reed A.R. 2003. Pre-formed activated carbon matting derived from the pyrolysis of biomass natural fibre textile waste. *J. Anal. Appl. Pyrolysis*, 70, 563-577.
- Williams P.T., Reed A.R. 2004. High grade activated carbon matting derived from the chemical activation and pyrolysis of natural fibre textile waste. *J. Anal. Appl. Pyrolysis*, 71, 971-986.
- Windeatt J.H., Ross A.B., Williams P.T., Forster P.M., Nahil M.A., Singh S. 2014. Characteristics of biochars from crop residues: Potential for carbon sequestration and soil amendment. *J. Environ. Manag.* 146, 189-197.
- Yahya M.A., Al-Qodah Z., Ngah C.C.Z. 2015. Agricultural bio-waste materials as potential sustainable precursors used for activated carbon production: A review. *Renew. Sus. Energ. Rev.* 46, 218-235.
- Yalcin N., Sevine V. 2000. Studies of the surface area and porosity of activated carbons prepared from rice husks. *Carbon*, 38, 1943-1945.
- Xu X., Huang D., Zhao L., Kan Y., Cao X. 2016. Role of inherent inorganic constituents in SO₂ sorption ability of biochars derived from three biomass wastes. *Environ. Sci. Technol.* 50, 12957-12965.
- Zhang L.Q., Jiang H.T., Ma C. Dong Y. 2012. Microwave regeneration characteristics of activated carbon for flue gas desulphurisation. *J. Fuel Chem. Technol.* 40(11), 1366-1371.
- Zhao Y. Fang F., Xiao H.M., Feng Q.P., Xiong L.Y., Fu S.Y. 2015. Preparation of pore-size controllable activated carbon fibers from bamboo fibers with superior performance for xenon storage. *Chem. Eng. J.* 270, 528-534.

Figure Captions

Figure 1. The non-woven fibrous flax fabric material

Figure 2. Non-woven fibrous activated carbon fabric material produced by chemical activation via pyrolysis followed by activation using KOH.

Figure 3. Scanning electron microscope image of the activated carbon after chemical activation

Figure 4. Schematic diagram of the fixed-bed sulphur dioxide adsorption system.

Figure 5. DFT-N₂ (a) and DFT-CO₂ (b) micropore distribution of the produced activated carbons.

Figure 6. DFT-N₂ (a) and DFT-CO₂ (b) micropore distribution of the commercially activated carbons.

Figure 7: SO₂ breakthrough profiles in relation to char and activated carbons produced from flax non-woven activated carbon fabric and commercially obtained activated carbons.

Figure 8. Cumulative SO₂ adsorption in relation to char and activated carbons produced from flax non-woven activated carbon fabric and commercially obtained activated carbons.

Figure 9. Relationship between SO₂ adsorption and BET surface area.

Figure 10. Relationship between SO₂ adsorption and micropore volume with nitrogen adsorption (DR-N₂) and carbon dioxide adsorption (DR-CO₂) (** represents DR-CO₂ for the KOH chemically activated non-woven fabric activated carbons only).

Figure 11. SO₂ breakthrough profiles in relation to the KOH activated carbons produced at 800 °C from flax non-woven activated carbon fabric in relation to reactor temperature of 25 °C, 40 °C and 100 °C.

Figure 12. Cumulative SO₂ adsorption in relation to the KOH activated carbons produced at 800 °C from flax non-woven activated carbon fabric in relation to reactor temperature of 25 °C, 40 °C and 100 °C.

Figure 13. SO₂ breakthrough profiles in relation to the KOH activated carbons produced at 800 °C from flax non-woven activated carbon fabric in relation to inlet SO₂ concentrations of 750 ppm, 2500 ppm and 5000 ppm.

Figure 14. Cumulative SO₂ adsorption in relation to the KOH activated carbons produced at 800 °C from flax non-woven activated carbon fabric in relation to inlet SO₂ concentrations of 750 ppm, 2500 ppm and 5000 ppm.



Figure 1. The non-woven fibrous flax fabric material



Figure 2. Non-woven fibrous activated carbon fabric material produced by chemical activation via pyrolysis followed by activation using KOH.

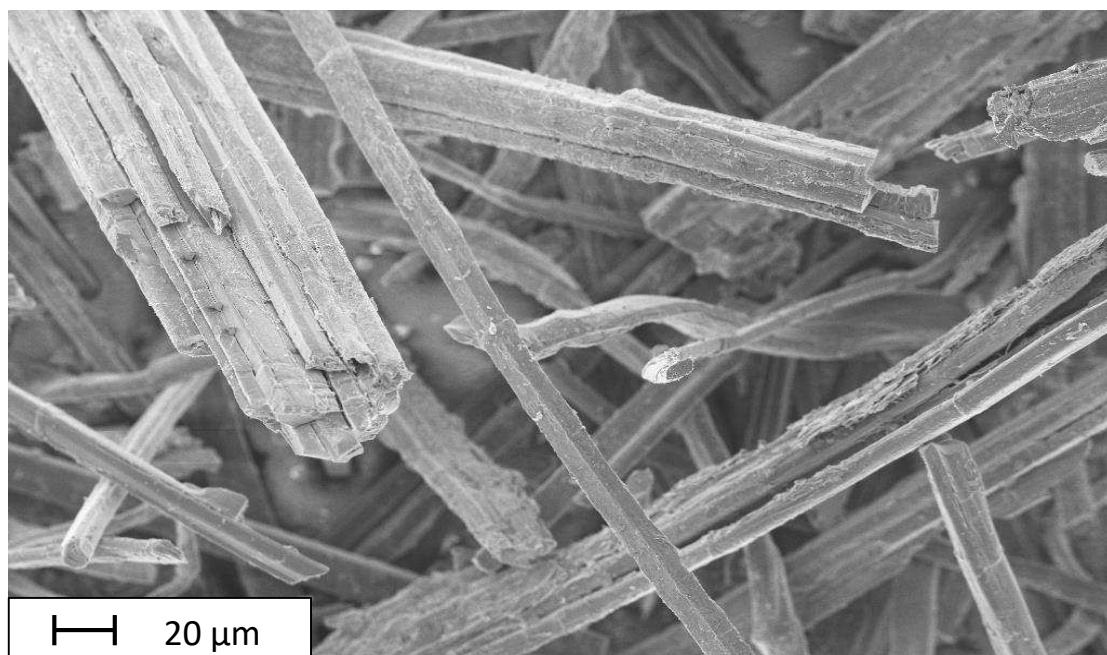


Figure 3. Scanning electron microscope image of the activated carbon after chemical activation

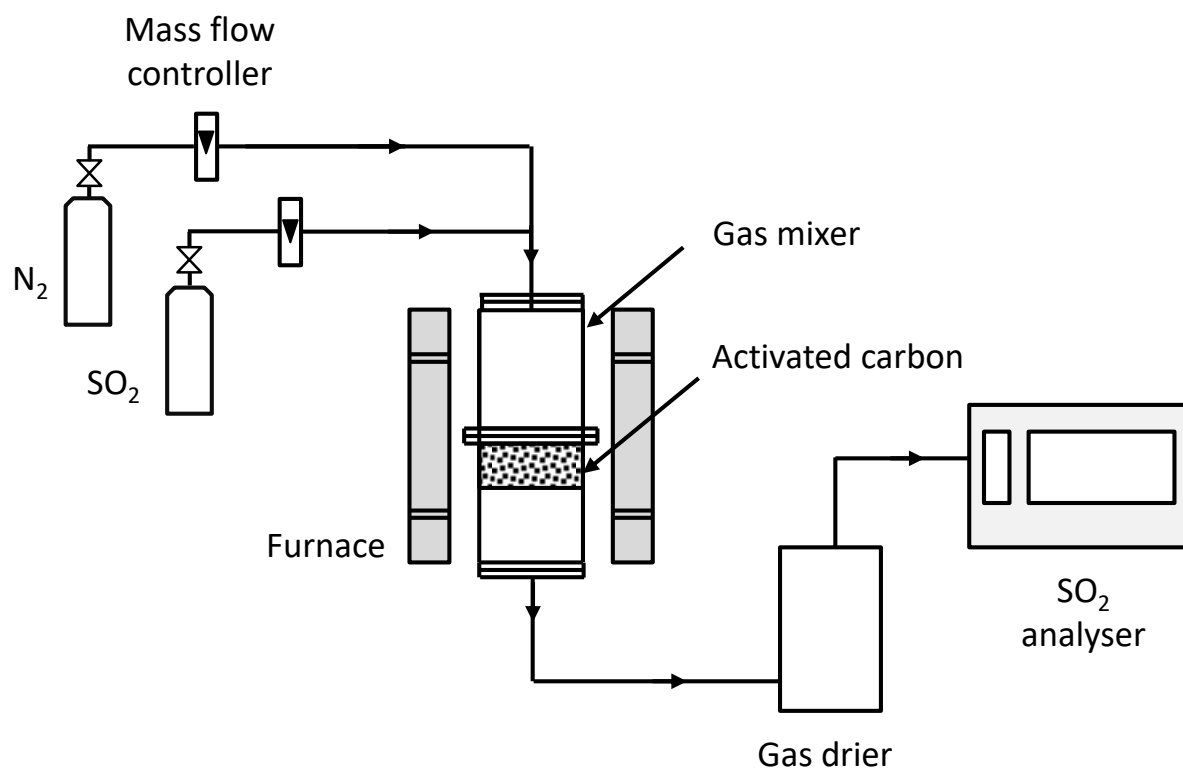


Figure 4. Schematic diagram of the fixed-bed sulphur dioxide adsorption system

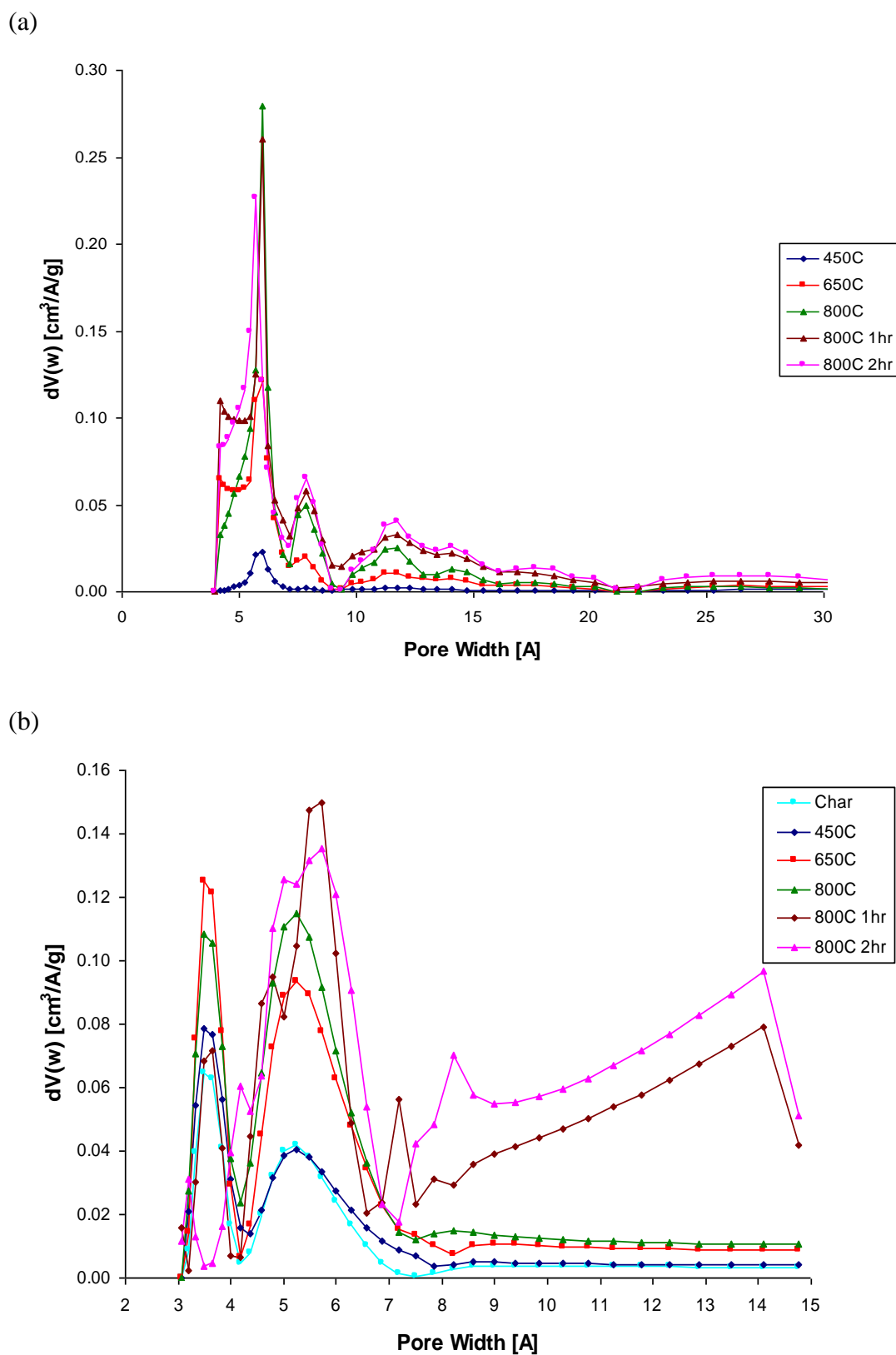


Figure 5. DFT-N₂ (a) and DFT-CO₂ (b) micropore distribution of the produced activated carbons.

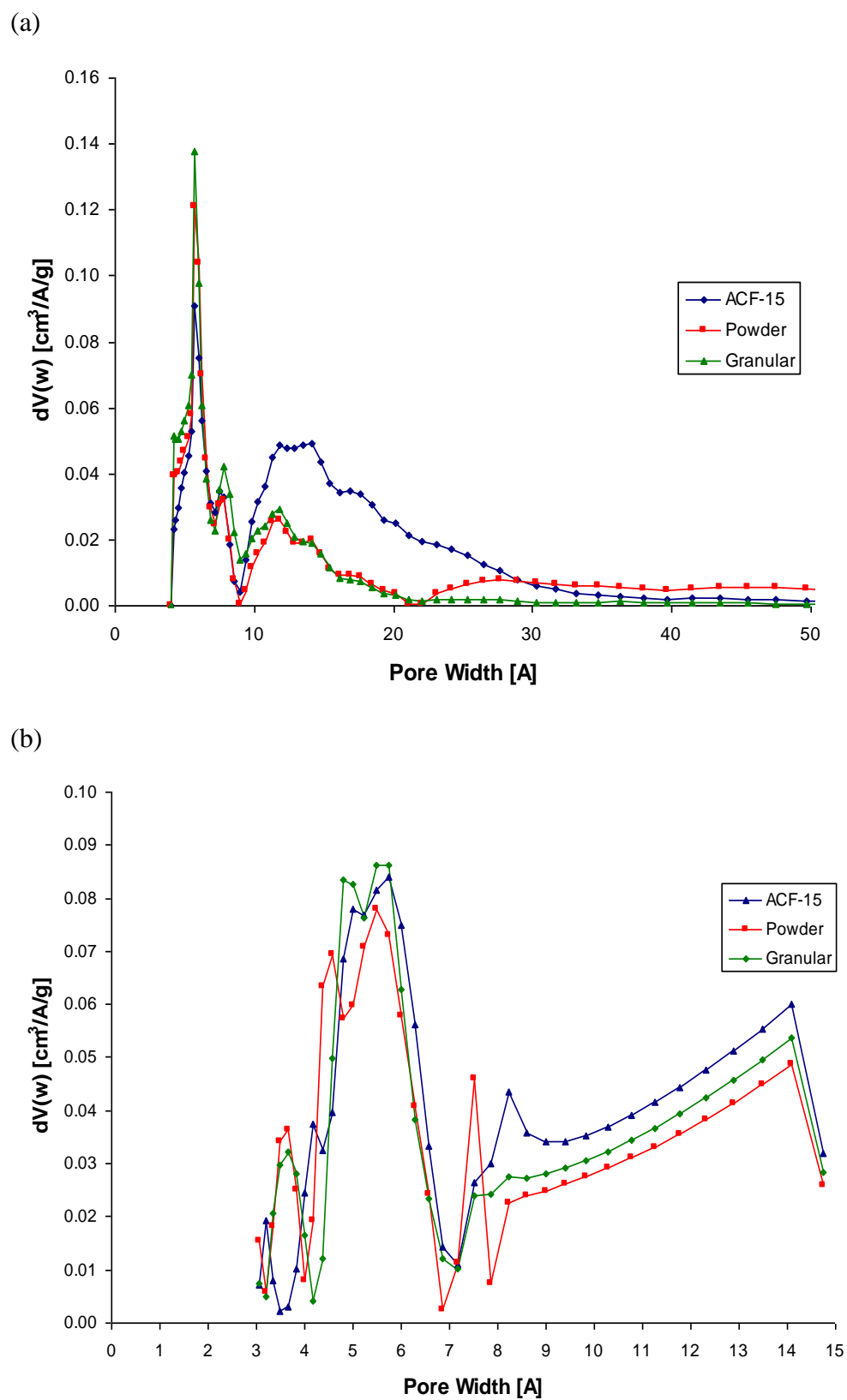


Figure 6. DFT- N_2 (a) and DFT- CO_2 (b) micropore distribution of the commercially activated carbons.

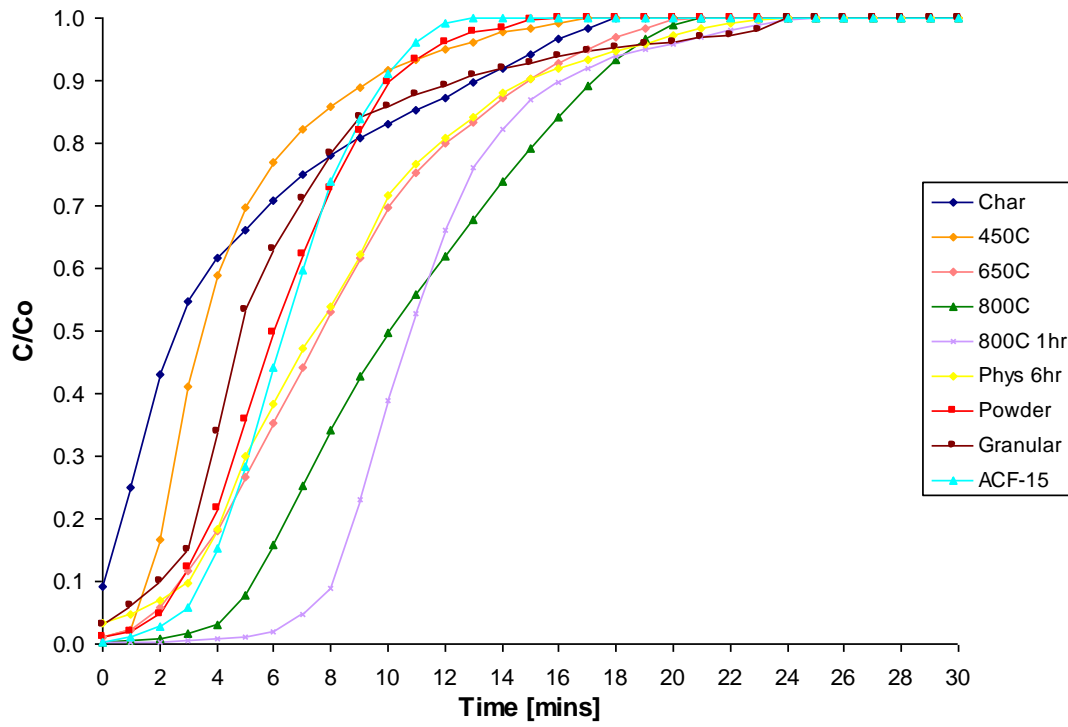


Figure 7: SO_2 breakthrough profiles in relation to char and activated carbons produced from flax non-woven activated carbon fabric and commercially obtained activated carbons.

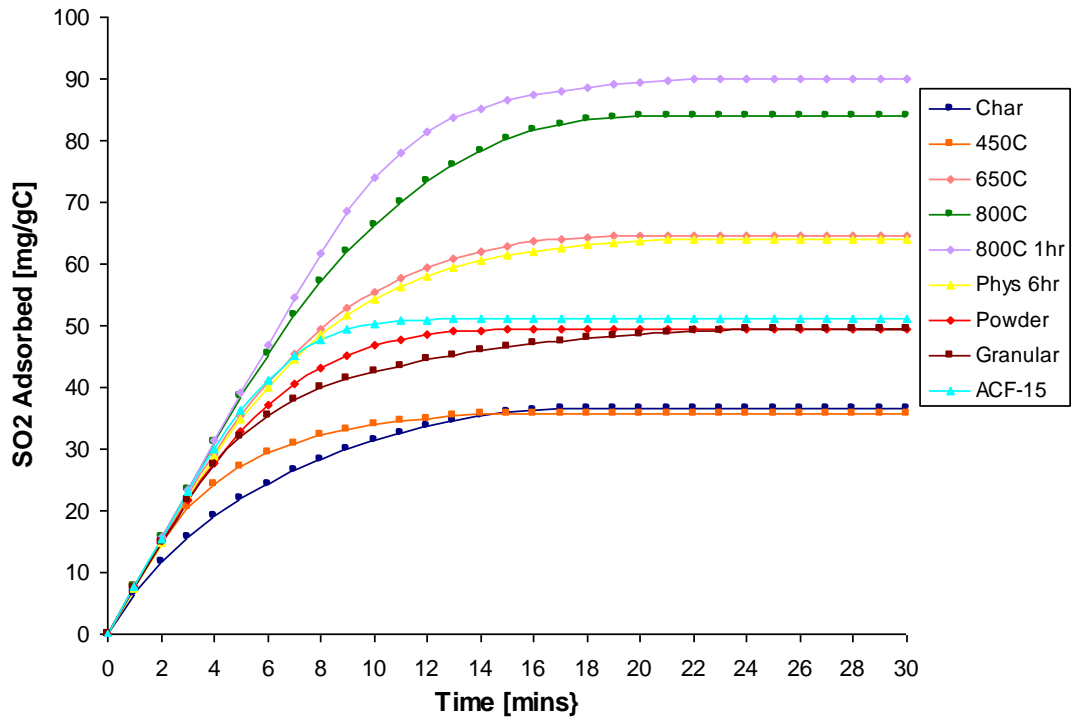


Figure 8. Cumulative SO₂ adsorption in relation to char and activated carbons produced from flax non-woven activated carbon fabric and commercially obtained activated carbons.

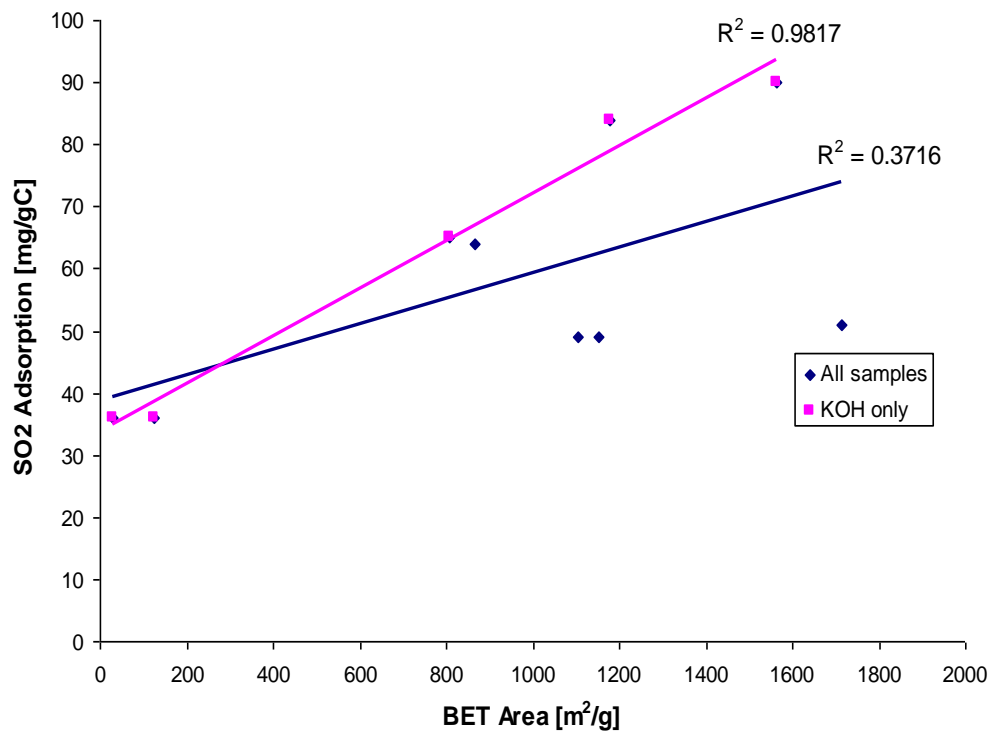


Figure 9. Relationship between SO₂ adsorption and BET surface area

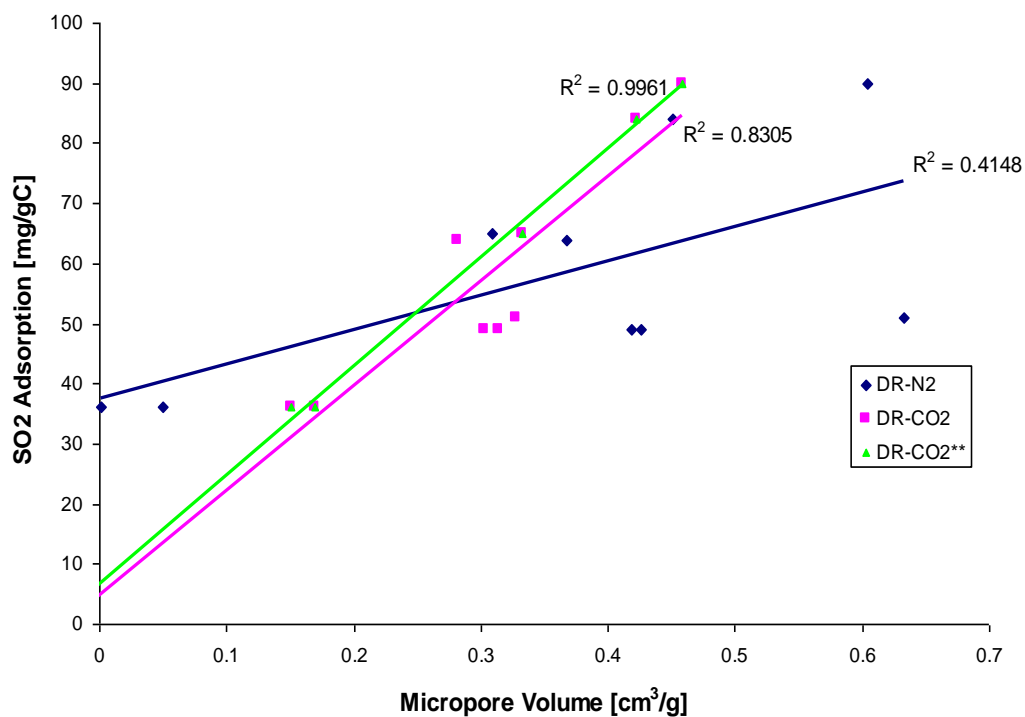


Figure 10. Relationship between SO₂ adsorption and micropore volume with nitrogen adsorption (DR-N₂) and carbon dioxide adsorption (DR-CO₂) (** represents DR-CO₂ for the KOH chemically activated non-woven fabric activated carbons only).

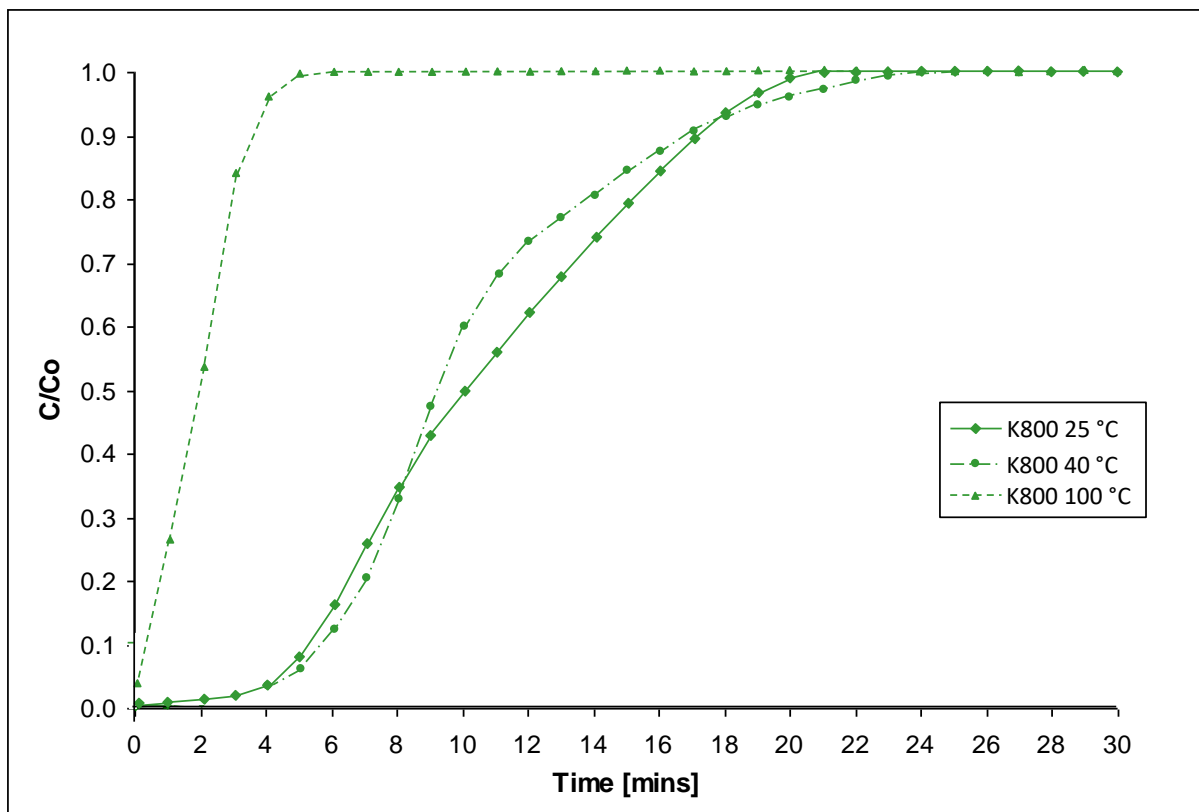


Figure 11. SO₂ breakthrough profiles in relation to the KOH activated carbons produced at 800 °C from flax non-woven activated carbon fabric in relation to reactor temperature of 25 °C, 40 °C and 100 °C.

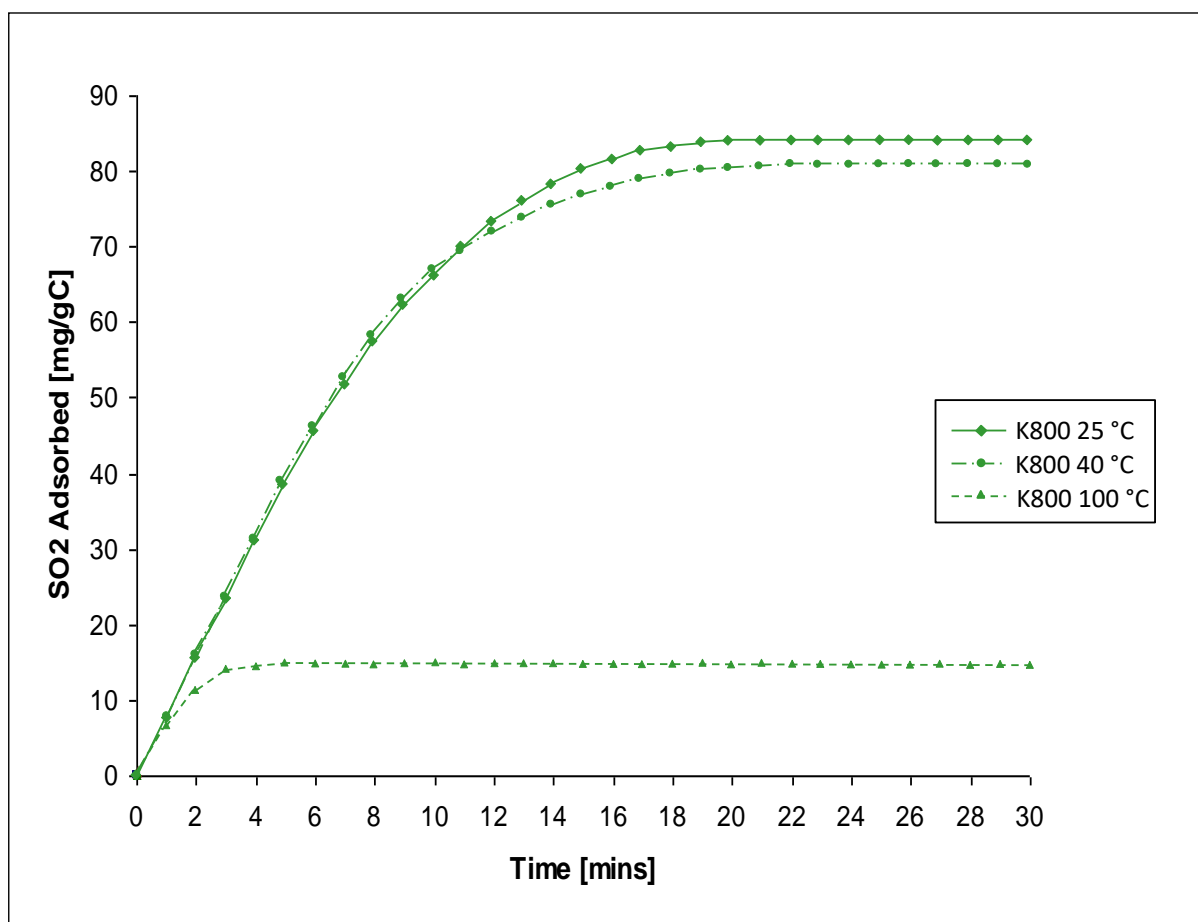


Figure 12. Cumulative SO₂ adsorption in relation to the KOH activated carbons produced at 800 °C from flax non-woven activated carbon fabric in relation to reactor temperature of 25 °C, 40 °C and 100 °C.

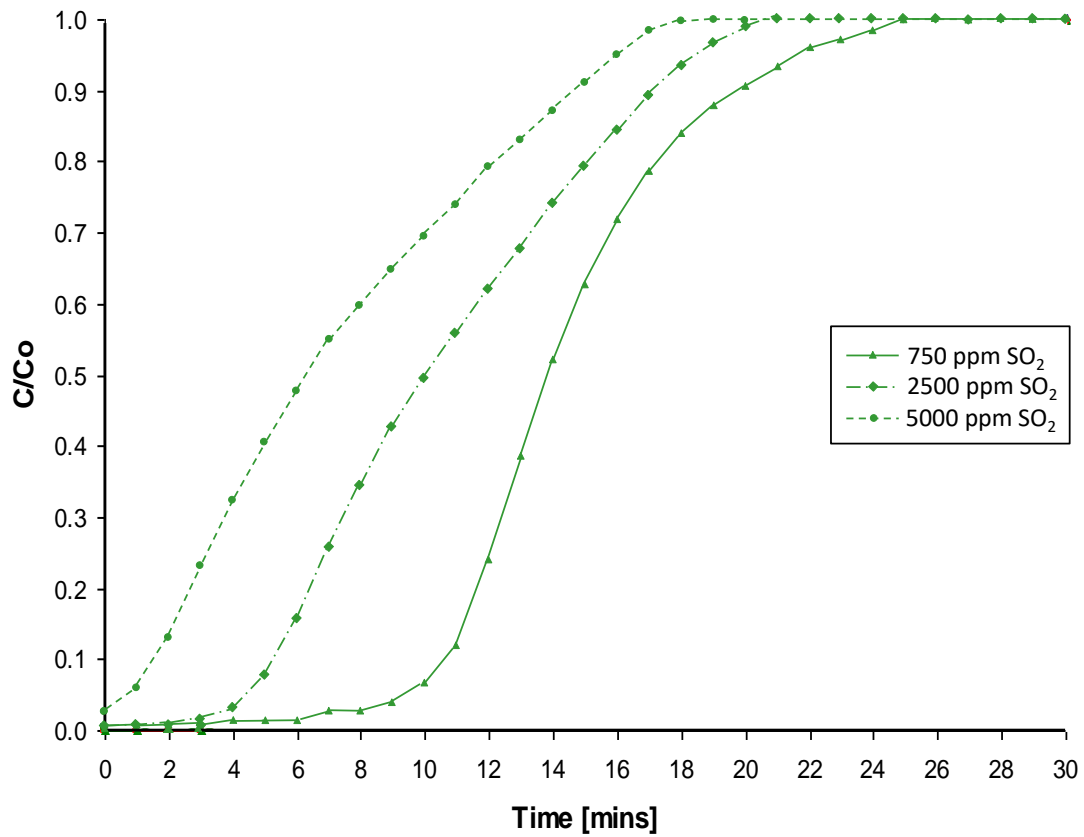


Figure 13. SO_2 breakthrough profiles in relation to the KOH activated carbons produced at 800 °C from flax non-woven activated carbon fabric in relation to inlet SO_2 concentrations of 750 ppm, 2500 ppm and 5000 ppm.

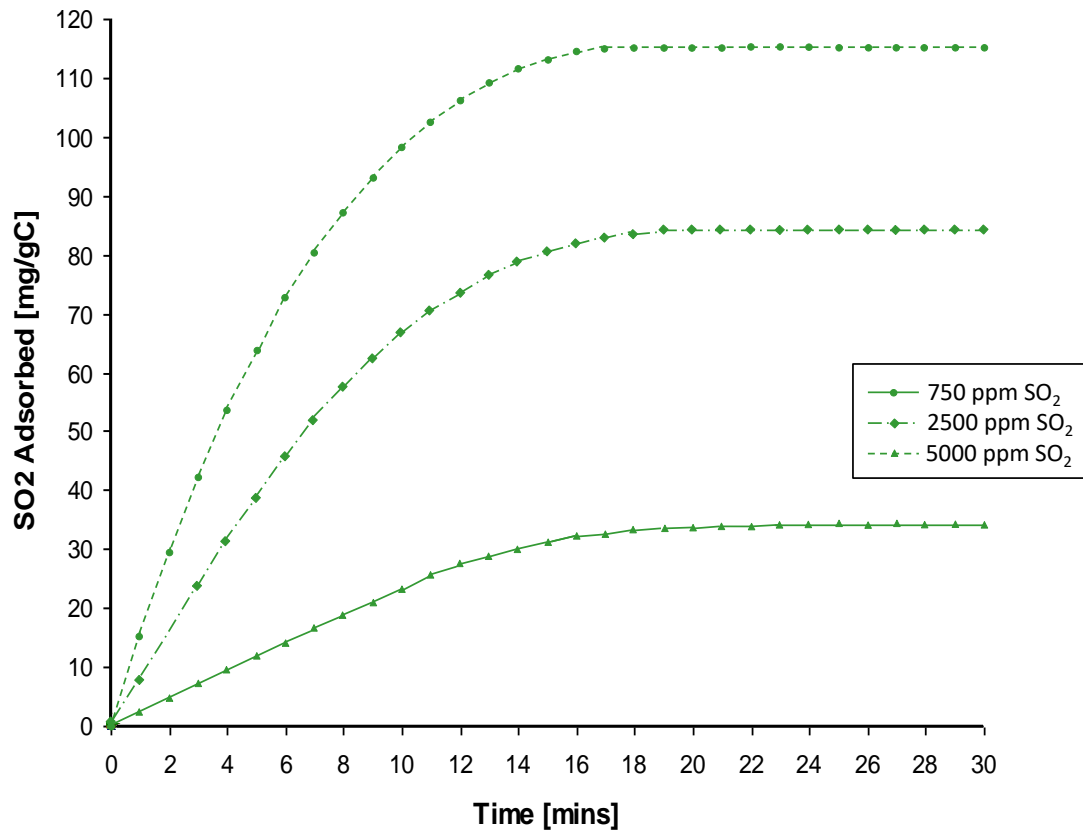


Figure 14. Cumulative SO₂ adsorption in relation to the KOH activated carbons produced at 800 °C from flax non-woven activated carbon fabric in relation to inlet SO₂ concentrations of 750 ppm, 2500 ppm and 5000 ppm.

Table 1. Properties of the activated carbons

Carbon Designation	Preparation	Surface area (m² g⁻¹)	Micropore Volume DR-N₂ (cm³ g⁻¹)	Micropore Volume DR-CO₂ (cm³ g⁻¹)	Yield (wt.%)
Char	No activation; Untreated pyrolysis char, 800 °C	30	0.012	0.151	-
450C	Chemical activation; KOH, at 450 °C, 0 h hold	126	0.050	0.170	98
650C	Chemical activation; KOH, at 650 °C, 0 h hold	807	0.309	0.332	94
800C	Chemical activation KOH, at 800 °C, 0 h hold	1177	0.451	0.422	83
800C 1 hr	Chemical activation; KOH, 800 °C, 1 h hold	1564	0.604	0.458	67
800C 2 hr	Chemical activation; KOH, 800 °C, 1 2 hold	1656	0.639	0.464	57
Phys 6hr	Physical activation; CO ₂ , 825 °C, 6 hr hold	867	0.337	0.281	40
Powder	Commercial activated carbon powder	1105	0.418	0.314	-
Granular	Commercial activated carbon granular	1154	0.426	0.303	-
ACF15	Commercial activated carbon fibre	1715	0.633	0.328	-